

Serum and Urine Metabolomic Profiling of Newly Diagnosed Treatment-Naïve Inflammatory Bowel Disease Patients

Laila Aldars-García, PhD,^{*} Rubén Gil-Redondo, MS,[†] Nieves Embade, PhD,[†] Sabino Riestra, MD,[‡] Montserrat Rivero, MD,[§] Ana Gutiérrez, MD, PhD,[¶] Iago Rodríguez-Lago, MD, PhD,^{||} Luis Fernández-Salazar, MD,^{**} Daniel Ceballos, MD,^{††, } José Manuel Benítez, MD,^{‡‡} Mariam Aguas, MD, PhD,^{§§} Iria Baston-Rey, MD,^{¶¶} Fernando Bermejo, MD, PhD,^{|||, } María José Casanova, MD, PhD,^{*} Rufo Lorente, MD,^{***} Yolanda Ber, MD,^{†††} Daniel Ginard, MD,^{‡‡‡} María Esteve, MD,^{§§§} Ruth de Francisco, MD,[‡] María José García, MD,[§] Rubén Francés, MD, PhD,^{**} Ainhoa Rodríguez Pescador, MD,^{||} Benito Velayos, MD,^{**} Elena Guerra del Río, MD,^{††} Sandra Marín Pedrosa, MD,^{‡‡} Alejandro Minguez Sabater, MD,^{§§} Manuel Barreiro-de Acosta, MD, PhD,^{¶¶} Alicia Algaba, PhD,^{|||} Cristina Verdejo Gil, MD,^{***} Olga Rivas, MD,^{†††} Vanesa Royo, MD,^{‡‡‡} Montserrat Aceituno, MD,^{§§§} Ana Garre, MS,^{*} Montserrat Baldán-Martín, PhD,^{*} Cristina Ramírez, BS,^{*} Ancor Sanz-García, PhD,^{||||} Juan J. Lozano, PhD,^{****} Julia Sidorova, PhD,^{****} Oscar Millet, PhD,[†] David Bernardo, PhD,^{††††, ‡‡‡‡} Javier P. Gisbert, MD, PhD,^{*, a} and María Chaparro, MD, PhD^{*, a, }

From the ^{*}Hospital Universitario de La Princesa, Instituto de Investigación Sanitaria del Hospital de La Princesa, Universidad Autónoma de Madrid, Centro de Investigación Biomédica en Red de Enfermedades Hepáticas y Digestivas, Madrid, Spain

[†]Precision Medicine and Metabolism Lab, CIC bioGUNE, Derio, Spain

[‡]Hospital Universitario Central de Asturias, Instituto de Investigación Sanitaria del Principado de Asturias, Oviedo, Spain

[§]Hospital Universitario Marqués de Valdecilla, Instituto de Investigación Sanitaria Marqués de Valdecilla, Santander, Spain

[¶]Hospital General Universitario de Alicante, Centro de Investigación Biomédica en Red de Enfermedades Hepáticas y Digestivas, Instituto Investigación Sanitaria y Biomédica de Alicante, Alicante, Spain

^{||}Hospital Universitario de Galdakao, Biocruces Bizkaia Health Research Institute, Vizcaya, Spain

^{**}Hospital Clínico Universitario de Valladolid, Valladolid, Spain

^{††}Hospital Universitario de Gran Canaria Dr. Negrín, Las Palmas de Gran Canaria, Spain

^{‡‡}Hospital Universitario Reina Sofía, Instituto Maimónides de Investigación Biomédica de Córdoba, Córdoba, Spain

^{§§}Hospital Universitari i Politecnic La Fe, La Fe Health Research Institute, Valencia, Spain

^{¶¶}Complejo Hospitalario Universitario de Santiago, Santiago de Compostela, Spain

^{|||}Hospital Universitario de Fuenlabrada, Instituto de Investigación Hospital Universitario La Paz, Madrid, Spain

^{***}Hospital General Universitario de Ciudad Real, Ciudad Real, Spain

^{†††}Hospital San Jorge, Huesca, Spain

^{‡‡‡}Hospital Universitari Son Espases, Palma de Mallorca, Spain

^{§§§}Hospital Universitari Mutua Terrassa, Centro de Investigación Biomédica en Red de Enfermedades Hepáticas y Digestivas, Terrassa, Spain

^{¶¶¶}Departamento Medicina Clínica, Universidad Miguel Hernández de Elche, Instituto de Investigación, Desarrollo e Innovación en Biotecnología Sanitaria de Elche, Universidad Miguel Hernández, Centro de Investigación Biomédica en Red de Enfermedades Hepáticas y Digestivas, Instituto Investigación Sanitaria y Biomédica de Alicante, Elche, Spain

^{|||}Data Analysis Unit, Hospital Universitario de La Princesa, Instituto de Investigación Sanitaria del Hospital Universitario de La Princesa, Madrid, Spain

^{****}Bioinformatics Platform, Centro de Investigación Biomédica en Red de Enfermedades Hepáticas y Digestivas, Barcelona, Spain

^{††††}Mucosal Immunology Lab, Unidad de Excelencia Instituto de Biología y Genética Molecular, Universidad de Valladolid, Consejo Superior de Investigaciones Científicas (CSIC), Valladolid, Spain

^{‡‡‡‡}Centro de Investigación Biomédica en Red de Enfermedades Infecciosas, Madrid, Spain

^aCo-senior authors. **Address correspondence to:** María Chaparro, MD, PhD, Inflammatory Bowel Disease Unit, Department of Gastroenterology, Hospital Universitario de La Princesa, Diego de León, 62, 28006 Madrid, Spain (mariachs2005@gmail.com).

Background and Aims: Inflammatory bowel disease (IBD) is a prevalent chronic noncurable disease associated with profound metabolic changes. The discovery of novel molecular indicators for unraveling IBD etiopathogenesis and the diagnosis and prognosis of IBD is therefore pivotal. We sought to determine the distinctive metabolic signatures from the different IBD subgroups before treatment initiation.

Methods: Serum and urine samples from newly diagnosed treatment-naïve IBD patients and age and sex-matched healthy control (HC) individuals were investigated using proton nuclear magnetic resonance spectroscopy. Metabolic differences were identified based on univariate and multivariate statistical analyses.

Results: A total of 137 Crohn's disease patients, 202 ulcerative colitis patients, and 338 HC individuals were included. In the IBD cohort, several distinguishable metabolites were detected within each subgroup comparison. Most of the differences revealed alterations in energy and amino acid metabolism in IBD patients, with an increased demand of the body for energy mainly through the ketone bodies. As compared with HC individuals, differences in metabolites were more marked and numerous in Crohn's disease than in ulcerative colitis patients, and in serum than in urine. In addition, clustering analysis revealed 3 distinct patient profiles with notable differences among them based on the analysis of their clinical, anthropometric, and metabolomic variables. However, relevant phenotypical differences were not found among these 3 clusters.

Conclusions: This study highlights the molecular alterations present within the different subgroups of newly diagnosed treatment-naïve IBD patients. The metabolomic profile of these patients may provide further understanding of pathogenic mechanisms of IBD subgroups. Serum metabolite seemed to be especially sensitive to the onset of IBD.

Key Words: inflammatory bowel disease., Crohn's disease, ulcerative colitis, metabolomics

WHAT IS KNOWN—Inflammatory bowel disease (IBD) is the result of a complex interaction among different factors. Novel molecular indicators may help in IBD understanding.

WHAT IS NEW HERE—We analyzed a large cohort of newly diagnosed IBD patients (before starting any treatment). At disease onset, IBD patients have significant metabolomic differences compared with control individuals; most of the differences revealed alterations in energy and amino acid metabolism.

HOW CAN THIS STUDY HELP PATIENT CARE? In-depth characterization of IBD patients is needed to understand the disease and propose therapeutic targets. This research could help in patient stratification, based on their metabolomic profile in different matrices, according to their specific IBD characteristics in order to improve the clinical approach.

Introduction

Inflammatory bowel diseases (IBDs) encompass a group of chronic inflammatory bowel pathologies of idiopathic origin that affect millions of people throughout the world. The 2 most important pathologies covered by this term are Crohn's disease (CD) and ulcerative colitis (UC),¹ which are not curable and show a chronic evolution with flares, alternating periods in remission, and relapses. In Europe and North America, over 2 and 1.5 million people experience the disease, respectively, having highest incidence rates and prevalence of IBD worldwide.^{2,3}

The use of metabolomics redefines disease understanding and phenotyping of clinical characteristics in many medical disorders. Metabolomics offers a holistic approach in the determination of metabolites in a biological system, and the omics method is most closely related to an individual phenotype.⁴ This is particularly relevant for IBD, in which a deeper understanding of its pathogenesis could lead to novel integrated therapies and contribute to the development of personalized disease management.

IBD diagnosis requires an invasive procedure, and CD and UC are also usually diagnosed too late, when severe complications have already occurred.⁵ Therefore, novel and noninvasive diagnostic indicators with more accurate discrimination potential would have a direct and high impact on the improvement of IBD outcomes. In this regard, metabolomics analysis in noninvasive accessible biological samples

such as blood and urine would definitively help to meet this challenge.

The early diagnosis of IBD is crucial for timely and effective treatment, and biomarkers for disease classification are needed. The differential diagnosis between UC and CD is also essential because distinct approaches regarding therapeutic and surgical treatment are needed. Moreover, both CD and UC differ from each other in terms of prognosis and tendency for recurrence. It is widely reported that the serological and urinary metabolomic profile could be used to separate subjects with IBD from those without IBD.⁶ However, from the clinical point of view, patient stratification based on metabolomic analyses within different IBD subgroups, including differences in disease severity and location, are still beyond our reach. Moreover, most of the published studies had certain limitations, such as small cohort sizes, cohorts with an established and long-lasting disease, lack of prospective data, different disease activities, and influence of treatment interventions. Therefore, we aimed to identify metabolites associated with onset IBD subgroups, including the different disease severities and locations in a unique large cohort of newly diagnosed IBD patients without any treatment interventions related to the disease.

Hence, and to overcome these limitations, we aimed to identify novel metabolites associated with IBD subgroups at onset, considering not only disease type (CD and UC), but also disease severity and location of the inflammation in a unique large cohort of newly diagnosed IBD patients without any treatment interventions related to the disease. We therefore consider that our novel results provide a comprehensive understanding of IBD beyond its classical criteria at the time that could also improve its diagnose and prognosis in a non-invasive manner.

Methods

Ethics

The study was conducted according to the Declaration of Helsinki. All experimental procedures were approved by the Ethics Research Committee of the coordinating hospital (Hospital Universitario de La Princesa, Madrid, Spain). Informed consent was obtained from all participants, and protocols were reviewed and approved by local institutional review boards. All data were anonymized to protect the confidentiality of participants.

Study design

The current study was part of a larger project designed to characterize newly diagnosed, treatment-naïve patients from a multiomic perspective, the IBDomics study. IBDomics is a prospective, multicenter, cohort study of adult patients diagnosed with IBD (CD, UC, or unclassified IBD) during 18 months in Spain. In this project, each incident case was followed for 1 year to determine changes in disease phenotype or location, the need for treatments, and the need for hospital admission or surgery. The present study included the metabolomic study of the basal serum and urine samples.

Study Population and Sample Collection

IBD patients

The cohort includes patients >18 years of age with IBD (CD or UC) diagnosed by colonoscopy during 2017 to 2019 in 16 hospitals in Spain according to the European Crohn's and Colitis Organization criteria. Patients with more than 1 month after the first IBD diagnosis, those who had started any treatment for IBD prior to the baseline, those receiving immunosuppressive treatment for any pathology other than IBD, those with an immune-mediated disease different from IBD, those who had a neoplasm or an active infection, and pregnant or lactating women were excluded.

Fasting urine and serum samples were collected at diagnosis (recruiting date, without treatment). Written informed consent was obtained from each participant prior to enrolment.

Control Individuals

Urine and serum samples from 338 healthy control (HC) individuals were provided by the Basque Biobank for research. They all were adults (18-70 years of age) matched for sex, age, body mass index, and smoking habit to the IBD subjects. The same exclusion criteria were applied to the control cohort, and none of the donors reported IBD problems or any related digestive problems.

Sample Preparation for Proton Nuclear Magnetic Resonance Spectroscopy

Urine samples were kept at 4 °C immediately after collection and aliquoted and stored at -80 °C until further analysis. The day of the analysis, samples were defrosted at room temperature. All the tubes were centrifuged at 1500 g for 5 minutes at 4 °C to remove urine debris. A total of 630 µL of the supernatant was transferred into a 1.5-mL Eppendorf tube containing 70 µL of a phosphate buffer (1.5 M $\text{KH}_2\text{PO}_4/\text{K}_2\text{HPO}_4$, 2 mM NaN_3 , 1% trimethylsilylpropionic acid- d_4 sodium salt or TSP in 70% D_2O , pH 7.4). This mix containing urine and buffer was vortexed, and 600 µL of the mixture was transferred into a 5 mm proton nuclear magnetic resonance spectroscopy (^1H -NMR) tube. The ^1H -NMR tubes were stored at 5 °C inside a tempered SampleJet automatic sample changer mounted on a 600 MHz IVDr spectrometer (Bruker Biospin).

Blood samples were collected and serum was obtained after centrifugation at 1500 g for 15 minutes. Serum aliquots were stored at -80 °C until measured. The day of the analysis, frozen samples were individually thawed at room temperature for 15 minutes. ^1H -NMR samples were then prepared using a SamplePro Tube (Bruker Biospin) robot system for liquid handling with integrated temperature control. Briefly, the robot automatically mixed every sample 1:1 (v/v) ratio with phosphate buffer (75 mM Na_2HPO_4 , 2 mM NaN_3 , 4.6

mM TSP in 80% D_2O , pH 7.4). The robot filled 5 mm ^1H -NMR tubes with 600 µL of the mix. After manually shaking every sample for several seconds, the ^1H -NMR tubes were stored at 5 °C inside a tempered SampleJet automatic sample changer mounted on a 600 MHz IVDr spectrometer.

^1H -NMR Analysis

All the experiments were measured using a 600 MHz Avance III spectrometer (Bruker Biospin), equipped with a BBI probe head with a z gradient coil and automatic tuning and matching. Every day, the spectrometer was calibrated following strict standard operation procedures in order to reach the highest spectral quality and reproducibility.^{7,8}

The ^1H -NMR spectra were measured at 300 K for urine and were referenced to the TSP signal (0 ppm). Two complementary experiments were recorded per sample: a 1-dimensional ^1H spectrum with water presaturation and long interscan recovery delay ($d1 = 10$ seconds) for metabolite quantification and a 2-dimensional J-resolved ^1H spectrum for helping on the metabolite identification. All spectra were acquired and processed with TopSpin3.5 (Bruker Biospin).

For serum analysis, 3 different experiments were carried out in automation mode per serum sample: a standard 1-dimensional experiment with solvent presaturation with gradient, a Carr-Purcell-Meiboom-Gill spin-echo experiment implementing a T2 filter to suppress the broad signals of proteins and other macromolecules, and a 2-dimensional J-resolved experiment.

Metabolite and lipoprotein quantification

Absolute quantifications from ^1H -NMR spectra were performed with Bruker IVDr software: B.I.Quant-UR E.1.1.0 for urine metabolites (mmol/L), B.I.Quant-PS 2.0.0 for serum metabolites (mmol/L), and B.I.LISA (Lipoprotein Subclass Analysis) PL-5009-01/001 for serum lipoproteins (mg/dL, except particle numbers that are expressed as nmol/L and ratios that are dimensionless).

Compilation of the control cohort

The control cohort was built-up from a large Spanish cohort including 10 000 donors that belong to the working population of the Basque Country. First, each 1-dimensional ^1H -NMR spectrum for each sample type (urine and serum) was segmented into consecutive buckets (bins) of fixed 0.03-ppm spectral width in the range between 0.5 and 9.5 ppm. Each bin was represented as the average intensity of their internal spectral points and normalized by the total spectrum intensity. The region between 4.7 and 5.00 (residual water) was excluded. Urine samples and serum samples were analyzed independently through a multivariate (bins) clustering algorithm, DBSCAN (density-based spatial clustering of applications with noise), in order to detect and remove extreme individuals (groups with low density or isolated samples). Bins were used as input variables after Pareto scaling. Input parameters for algorithm (from the dbscan R package, version 1.1-6 [R Foundation for Statistical Computing, R version 4-3-1]) were the following: $\text{eps} = 10$ (epsilon neighborhood size) and $\text{minPts} = 5$ (number of minimum points per eps region). Finally, 338 individuals were selected from the remaining cohort in a way that replicated a similar sex, age, body mass index, and smoking habit distributions when compared with IBD cohort.

Statistical Analysis of Urinary and Serum Metabolites/Lipoproteins

Data analysis

Each metabolite or lipoprotein subclass was compared between the control group and among the IBD subgroups through multivariable general linear models, using the metabolite/lipoprotein as dependent variable and the subgroup name as the independent variable, adjusting by sex, age, body mass index, and smoker habit. We used a linear regression model, as it allows to evaluate each metabolite/lipoprotein individually and the adjustment for covariates. As each metabolite/lipoprotein has a different scale, we presented the changes in number of standard deviations to make them comparable, taking as a reference the standard deviation of that metabolite in the control cohort (Figures 1, 2, 3, 4, 5, and 6). The first subgroup (control cohort) was chosen as reference. Estimates for the rest of subgroups were taken as effect size values after normalizing them by the standard deviation of the reference subgroup to make values comparable between metabolites/lipoproteins. Comparisons were summarized with forest plots (ggforestplot R package, version 0.1.0) in which significant/nonsignificant effect sizes were represented with closed/open points and standard errors as horizontal bars. The significance of a test for a given compound was determined by the Benjamini-Hochberg correction that controls for false discovery rate. In addition, the areas under the curve \pm 95% confidence interval were calculated for each compound in each comparison (Supplementary Tables 1 and 2).

Identification of data cluster structures

To further explore the structure of the data, an exploratory approach was conducted to determine clinical subphenotypes. For this purpose, continuous anthropometric and clinical measures of patients were identified and z -score normalized in order to feed them to principal component analyses (PCAs). The MATLAB (The MathWorks, MATLAB R2019b) built in *pca* function was used to perform the analysis. The PCA-derived simplified matrix was then used to define subphenotypes of IBD patients objectively through hierarchical clustering. Hierarchical clustering was performed using the R package *phreatmap* to conduct the analyses with parameters Euclidean distance as distance metric and complete-linkage as linkage criteria. Orthogonal projections to latent structures discriminant analysis models were trained using metabolomic data from blood and urine metabolites separately using the clusters of patients derived from hierarchical clustering as class labels. From the models, identification of most relevant metabolites was conducted using the variable importance parameter metric, with metabolites scoring a variable importance parameter >1 regarded as relevant by convention. Assessment of the model's quality was established through the $R^2X(\text{cum})$, $R^2Y(\text{cum})$, and $Q^2(\text{cum})$ metrics, which account for the cumulative modelled variation of the metabolites (R^2X), class labels (R^2Y), and the cross-validated predictive capability of the model (Q^2) after 7-fold cross-validation, which also helped to determine the number of orthogonal components. Models were constructed using the R package *ropls*, with Q^2 and R^2 statistical significance determined after permutation testing set at 100 iterations.

Results

Cohort Characteristics

We analyzed serum and urine samples from a total of 339 newly diagnosed treatment-naïve IBD patients and 338 HC individuals by $^1\text{H-NMR}$ spectroscopy. The main characteristics of the IBD patients and HC individuals are shown in Table 1. There were no significant differences in age or sex between patients and HC individuals. A panel of 150 urinary metabolites, 41 serum metabolites, and 112 serum lipoprotein subfractions, were identified using $^1\text{H-NMR}$ spectroscopy. The $^1\text{H-NMR}$ spectrum also allows a detailed characterization of the different lipoprotein subclasses.

Table 2 summarizes the differently abundant metabolites in serum and urine in all IBD subgroups compared with HC individuals and within IBD subgroups based on regression models adjusted for covariates. As compared with HC individuals, differences in metabolites were more marked in CD than in UC and in serum than in urine.

Serum and Urine Metabolite Profiling Unravels Alterations in Energy and Amino Acid Metabolism in IBD Patients

In serum, one of the main traits observed is the alteration in metabolites related with the energy metabolism. 2-Hydroxybutyric acid and ketone bodies (acetoacetic acid, 3-hydroxybutyric acid, and acetone) were significantly increased in serum IBD patients. Consistently with these results, serum glucose is also increased in IBD patients (Figure 1). The increase in succinic acid and pyruvic acid and decrease glutamic acid (Table 2), may all be related to this dysregulation of central carbon metabolism in the liver. We detected a significant reduction in essential amino acids such as leucine, lysine, methionine, phenylalanine, threonine, and valine along with a reduction in nonessential amino acids, including alanine, asparagine, glutamic acid, histidine (only essential in childhood), and tyrosine. In addition, increased level of serum's creatine in IBD patients was observed as well as a decrease in methionine and glycine.

Referred to the urine, the regression analysis revealed a total of 3 metabolites significantly different between CD and UC (Figure 2B and Table 2). These metabolites were 4-hydroxyphenylacetic (gut microbiota derived), citric acid (tricarboxylic acid [TCA] cycle intermediate), and L-tryptophan (Trp) (amino acid). Citric acid is significantly decreased in CD compared with UC as well as with HC individuals, whereas in UC there is no difference compared with HC individuals. On the contrary, 4-hydroxyphenylacetic is significantly increased in CD compared with UC as well as with HC individuals (Figure 2A), whereas in UC there is no difference compared with HC individuals. Therefore, they could act as pivotal urinary descriptors for the segregation of CD patients from the UC patients (Table 2).

Acetone, L-isoleucine, maleic acid, and succinic acid were significantly altered in UC urine but not in CD. Especially, succinic acid was sharply increased in UC patients. 2-Methylsuccinic acid, 4-hydroxyphenylacetic acid, D-mannitol, oxaloacetic acid, and pyruvic acid are only increased in CD patients, while acetone, L-isoleucine, L-citramalic acid, maleic acid, and prominently, succinic acid were only increased in UC patients' urine (Figure 2A). Such differences between CD and UC highlights the underlying

Table 1. Cohort characteristics.

	CD (n = 137)	UC (n = 202)	HC (n = 338)
Sex			
Male	70	104	176
Female	67	98	162
Onset age, y			
Mean	40.4	42.85	40.83
Range	18-84	19-82	19-66
Mean BMI, kg/m ²	24.49	25.15	25.02
Smoking habit^a			
Yes	45	21	67
No	92	180	271
CD location (Montreal)			
L1 (ileal) + L4 (upper intestinal)	70	—	—
L2 (colonic)	27	—	—
L3 (ileocolonic)	39	—	—
CD phenotype			
B1 (inflammatory)	122	—	—
B2 (stricturing)	7	—	—
B3 (penetrating)	7	—	—
p (perianal disease)**	19	—	—
CD severity (SES-CD)			
0-2	27	—	—
3-6	62	—	—
7-15	26	—	—
≥16	10	—	—
UC location			
E1 ulcerative proctitis	—	72	—
E2 left-sided UC	—	84	—
E3 extensive UC	—	56	—
UC severity			
Mild	—	46	—
Moderate	—	138	—
Severe	—	31	—
Extraintestinal manifestations			
Yes	15	18	—
No	117	182	—

Values are n, unless otherwise indicated.

Abbreviations: BMI, body mass index; CD, Crohn's disease; HC, healthy control; SES-CD, Simple Endoscopic Score for Crohn's Disease; UC, ulcerative colitis.

*P value <.05.

^bWithin the other phenotypes.

pathophysiological mechanisms that are believed to differ significantly between these 2 IBD subgroups.

Even though the previously mentioned metabolites altered in urine were related to energy and amino acid metabolism, this matrix rendered lower significance and a lower number of altered metabolites as compared with blood metabolites.

Lipoprotein Profiling Shows Alterations of Lipid Distribution in IBD Patients' Blood

The lipoprotein classes and subclasses in the different IBD subgroups, as analyzed by ¹H-NMR, are summarized in Supplementary Figures 1, 2, 3, 4, 5, 6, and 7. Clear alterations

of lipid distribution in IBD patients were observed. All changes more marked in CD than UC, as compared with HC individuals. Our findings are consistent with a triglyceride (TG)-rich lipoprotein profile in the IBD cohort: serum TG content and the mean concentration of TG-very low-density lipoproteins (LDLs) and TG-LDL. Inversely, total cholesterol, apolipoproteins (including Apo-A1, Apo-A2, and Apo-B), and phospholipids were decreased in IBD patients. Among these, the greatest decrease (by factor ca. 1.5) was observed for Apo-A2 (Supplementary Figure 1). This trend was observed for all IBD subgroups and was clearly marked in penetrating CD (Supplementary Figure 4), extensive UC, and more severe IBD (Supplementary Figures 5 and 7).

Table 2. Differential serum and urinary metabolites in all inflammatory bowel disease subtypes compared with HC individuals.

	Number of differential metabolites		Decreased		Increased	
	Urine	Serum	Urine	Serum metabolites	Urine	Serum metabolites
CD vs HC	21	25	Uracyl, hippuric acid, 1-methylnicotinamide, citric acid, trigonelline, allantoin, 1-methylhistidine, methanol, methylmalonic acid, taurine	Asparagine, citric acid, creatinine, dimethylsulfone, glutamic acid, glutamine, glycine, histidine, lactic acid, leucine, lysine, methionine, ornithine, tyrosine, valine	3-Hydroxyisovaleric acid, 4-hydroxyphenylacetic acid, orotic acid, 2-hydroxy-4-methylvaleric acid, 2-methylsuccinic acid, 4-pyridoxic acid, acetoacetic acid, oxaloacetic acid, d-mannitol, propylene glycol, pyruvic acid	2-Hydroxybutyric acid, 3-hydroxybutyric acid, acetoacetic acid, acetone, creatine, formic acid, glucose, proline, pyruvic acid, succinic acid
UC vs HC	14	26	Uracyl, hippuric acid, 1-methylnicotinamide, trigonelline	Asparagine, alanine, glutamic acid, glycerol, glycine, histidine, lactic acid, leucine, lysine, methionine, ornithine, phenylalanine, sarcosine, threonine, tyrosine, valine	Orotic acid, 4-pyridoxic acid, propylene glycol, L-citramalic acid, L-isoleucine, acetone, succinic acid, maleic acid, paracetamol-glucuronide	2-Hydroxybutyric acid, 3-hydroxybutyric acid, acetoacetic acid, acetone, creatine, formic acid, glucose, proline, pyruvic acid, succinic acid
CD vs UC	3	0	Citric acid	None	4-Hydroxyphenylacetic acid, L-tryptophan	None
CD severity	13	16	1-Methylnicotinamide, citric acid, hippuric acid, methylmalonic acid, uracyl	Asparagine, creatinine, glutamic acid, glycerol, histidine, K-EDTA, lactic acid, leucine, lysine, methionine, ornithine, valine	2-Methylsuccinic acid, 4-hydroxyphenylacetic acid, 4-pyridoxic acid, D-mannitol, N,N-dimethylglycine, orotic acid, oxaloacetic acid	Creatine, formic acid, glucose, proline
7-15	17	20	1-Methylnicotinamide, 2-oxoglutaric acid, citric acid, dimethylamine, hippuric acid, methylmalonic acid, thymol, trigonelline, uracyl	Asparagine, creatinine, glutamic acid, glutamine, histidine, lactic acid, leucine, lysine, methionine, ornithine	2-Hydroxy-4-methylvaleric acid, 2-methylsuccinic acid, 4-hydroxyphenylacetic acid, 4-pyridoxic acid, dihydrothymine, myo-inositol, paracetamol, propylene glycol	3-Hydroxybutyric acid, acetic acid, acetoacetic acid, acetone, creatine, formic acid, glucose, proline, pyruvic acid, succinic acid
>16	23	19	1-Methylnicotinamide, citric acid, hippuric acid, thymol, trigonelline, uracyl	Alanine, asparagine, citric acid, glutamic acid, histidine, lactic acid, leucine, lysine, methionine, ornithine	2-Hydroxy-4-methylvaleric acid, 2-methylsuccinic acid, 3-hydroxyisovaleric acid, 4-aminobutyric acid, 4-hydroxyhippuric acid, 4-hydroxyphenylacetic acid, 4-pyridoxic acid, acetoacetic acid, D-mannitol, galactitol, L-pyroglutamic acid, orotic acid, oxaloacetic acid, propionylglycine, pyruvic acid, quinolinic acid, succinic acid	2-Hydroxybutyric acid, 3-hydroxybutyric acid, acetoacetic acid, acetone, creatine, formic acid, glucose, proline, pyruvic acid, succinic acid
UC severity	2	13	Uracyl	Asparagine, creatinine, glutamic acid, glycine, histidine, lactic acid, methionine, ornithine,	Cystine	3-Hydroxybutyric acid, acetoacetic acid, creatine, formic acid, glucose
Mild	14	26	1-Methylnicotinamide, hippuric acid, trigonelline, uracyl	Alanine, asparagine, glutamic acid, glycerol, glycine, histidine, lactic acid, leucine, lysine, methionine, N,N-dimethylglycine, ornithine, phenylalanine, sarcosine, threonine, tyrosine, valine	3-Hydroxybutyric acid, 4-pyridoxic acid, acetone, L-citramalic acid, L-fucose, L-isoleucine, leucine, maleic acid, orotic acid, succinic acid	2-Hydroxybutyric acid, 3-hydroxybutyric acid, acetoacetic acid, acetone, formic acid, glucose, proline, pyruvic acid, succinic acid
Moderate	14	26	1-Methylnicotinamide, hippuric acid, trigonelline, uracyl	Alanine, asparagine, glutamic acid, glycerol, glycine, histidine, lactic acid, leucine, lysine, methionine, N,N-dimethylglycine, ornithine, phenylalanine, sarcosine, threonine, tyrosine, valine	3-Hydroxybutyric acid, 4-pyridoxic acid, acetone, L-citramalic acid, L-fucose, L-isoleucine, leucine, maleic acid, orotic acid, succinic acid	2-Hydroxybutyric acid, 3-hydroxybutyric acid, acetoacetic acid, acetone, formic acid, glucose, proline, pyruvic acid, succinic acid

Table 2. Continued

	Number of differential metabolites		Decreased		Increased	
	Urine	Serum	Urine	Serum metabolites	Urine	Serum metabolites
Severe	19	15	Trigonelline, uracil	Glutamic acid, histidine, lactic acid, leucine, lysine, ornithine, phenylalanine	1-Methylguanidine, 3-aminoisobutyric acid, 3-hydroxybutyric acid, acetoacetic acid, acetone, D-mannose, L-fucose, L-isoleucine, L-pyroglytamic acid, leucine, maleic acid, N-acetylaspartic acid, orotic acid, phenylacetic acid, propylene glycol, succinic acid, xanthurenic acid	3-Hydroxybutyric acid, acetone, creatine, formic acid, glucose, proline, pyruvic acid, succinic acid
CD location						
L1 (ileal) + L4 (upper-intestinal)	14	17	Allantoin, citric acid, hippuric acid, methylmalonic acid, trigonelline, uracil	Asparagine, creatinine, glutamic acid, histidine, lactic acid, leucine, lysine, methionine, ornithine	2-Methylsuccinic acid, 3-hydroxyisovaleric acid, 4-hydroxyphenylacetic acid, 4-pyridoxic acid, acetoacetic acid, D-mannitol, orotic acid, oxaloacetic acid	3-Hydroxybutyric acid, acetoacetic acid, acetone, creatine, formic acid, glucose, proline, pyruvic acid
L2 (colonic)	13	19	1-Methylnicotinamide, citric acid, hippuric acid, uracil	Asparagine, glutamic acid, glutamine, histidine, lactic acid, leucine, lysine, methionine, ornithine, phenylalanine, tyrosine, valine	2-Hydroxy-4-methylvaleric acid, 4-hydroxyphenylacetic acid, 4-pyridoxic acid, acetoacetic acid, dhydrothymine, L-pyroglytamic acid, maleic acid, paracetamol, propylene glycol	3-Hydroxybutyric acid, acetic acid, formic acid, ethanol, glucose, N,N-dimethylglycine, pyruvic acid
L3 (ileocolonic)	22	22	1-Methylnicotinamide, citric acid, hippuric acid, uracil, methanol, taurine, trigonelline, thymol	Acetic acid, asparagine, citric acid, creatinine, glutamic acid, glutamine, histidine, lactic acid, leucine, lysine, methionine, ornithine	2-Hydroxy-4-methylvaleric acid, 2-methylsuccinic acid, 4-hydroxyphenylacetic acid, 4-pyridoxic acid, acetoacetic acid, cytosine, D-mannitol, galactitol, N,N-dimethylglycine, orotic acid, oxaloacetic acid, propionylglycine, pyruvic acid, tyramine	2-Hydroxybutyric acid, 3-hydroxybutyric acid, acetoacetic acid, acetone, creatine, formic acid, glucose, N,N-dimethylglycine, proline, succinic acid
UC location						
E1 (proctitis)	1	14	Uracil	Asparagine, glutamic acid, glycerol, glycine, histidine, lactic acid, leucine, lysine, methionine, ornithine, phenylalanine	None	Acetoacetic acid, formic acid, glucose
E2 (left sided)	6	24	Uracil	Asparagine, glutamic acid, glycerol, glycine, histidine, lactic acid, leucine, lysine, methionine, N,N-dimethylglycine, ornithine, phenylalanine, threonine, valine	D-panthenol, leucine, maleic acid, methionine, orotic acid	2-hydroxybutyric acid, 3-hydroxybutyric acid, acetic acid, acetoacetic acid, acetone, creatine, formic acid, glucose, proline, pyruvic acid
E3 (extensive)	28	20	1-methylnicotinamide, citric acid, hippuric acid, methylmalonic acid, taurine, trigonelline, uracil	Alanine, asparagine, glutamic acid, glycine, histidine, lactic acid, lysine, methionine, ornithine, tyrosine	2-hydroxyisovaleric acid, 3-aminoisobutyric acid, 3-hydroxybutyric acid, 3-hydroxyglutaric acid, 4-pyridoxic acid, acetoacetic acid, acetone, allopurinol, L-citramalic acid, L-fucose, L-isoleucine, L-pyroglytamic acid, leucine, maleic acid, N-acetylaspartic acid, orotic acid, paracetamol-glucuronide, phenylacetic acid, propylene glycol, succinic acid, xanthurenic acid	2-Hydroxybutyric acid, 3-hydroxybutyric acid, acetoacetic acid, acetone, creatine, formic acid, glucose, proline, pyruvic acid, succinic acid

Table 2. Continued

CD phenotype	Number of differential metabolites		Decreased		Increased	
	Urine	Serum	Urine	Serum metabolites	Urine	Serum metabolites
B1 (inflammatory)	21	21	1-Methylnicotinamide, 2-oxoglutaric acid, allantoin, citric acid, hippuric acid, L-threonine acid, methanol, methylmalonic acid, pantothenic acid, thymol, trigonelline, uracil	Asparagine, creatinine, glutamic acid, glycine, histidine, lactic acid, leucine, lysine, methionine, ornithine, tyrosine, valine	2-Hydroxy-4-methylvaleric acid, 2-methylsuccinic acid, 4-hydroxyphenylacetic acid, 4-pyridoxic acid, acetoacetic acid, D-mannitol, propylene glycol, orotic acid, oxaloacetic acid	3-Hydroxybutyric acid, acetoacetic acid, acetone, creatine, formic acid, glucose, proline, pyruvic acid
B2 (stricturing)	5	6	None	Lactic acid	3-Methylglutaconic acid, choline, leucine, myo-inositol, sarcosine	2-Hydroxybutyric acid, 3-hydroxybutyric acid, acetoacetic acid, formic acid, succinic acid
B3 (penetrating)	18	11	Uracil	Alanine, asparagine, histidine, lactic acid, leucine, methionine	2-Hydroxyisovaleric acid, 2-methylsuccinic acid, 3-hydroxybutyric acid, 3-hydroxyisovaleric acid, 3-phenyllactic acid, 4-hydroxyphenylacetic acid, 4-pyridoxic acid, acetoacetic acid, adenine, D-mannitol, L-fucose, orotic acid, oxaloacetic acid, paracetamol-glucuronide, propionylglycine, pyruvic acid, theobromine	3-Hydroxybutyric acid, acetoacetic acid, acetone, formic acid, succinic acid

Abbreviations: CD, Crohn's disease; HC, healthy control; UC, ulcerative colitis.

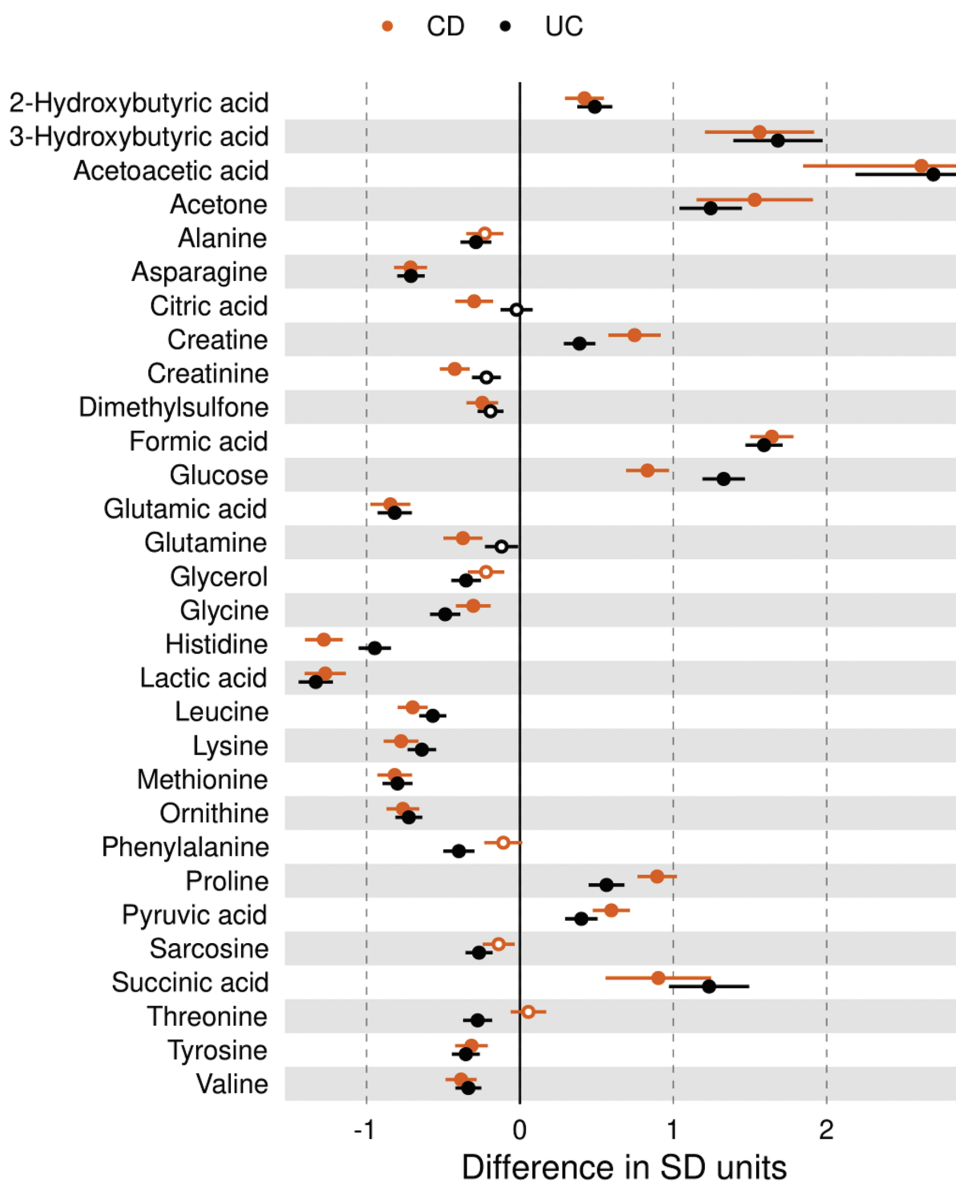


Figure 1. Changes in serum metabolites in Crohn's disease (CD) and ulcerative colitis (UC) patients compared with healthy control individuals. The horizontal axis is the number of standard deviations (SDs) that a metabolite is on average increased (or decreased) in inflammatory bowel disease (IBD) subtypes compared with healthy control individuals. Circles are positioned in the specific mean increase (decrease) value, whereas horizontal black bars are the 95% confidence interval. Statistically significant differences (P value $< .05$) are represented with filled circles.

Metabolomic profiles discriminate among IBD subgroups based on disease severity, location, and CD phenotype

Aiming to elucidate metabolomic differences among the different IBD subgroups (ie, disease severity and location for both the CD and UC phenotype), we conducted the statistical analysis also including the previously mentioned subgroups and results are shown in Figures 3, 4, 5, and 6 for serum and urinary metabolites.

Regarding CD severity, some urinary metabolites showed a segregated gradient based on disease severity, namely 2-hydroxy-4-methylvaleric acid, galactitol, quinolinic acid, and succinic acid (Figure 5C). In UC severity, urinary 3-aminoisobutyric acid, acetone, D-mannose, L-pyroglutamic acid, leucine, maleic acid, N-acetylaspargic acid, phenylacetic acid, propylene glycol, trigonelline, uracil, and xanthurenic

acid (Figure 6B) and serum ketone bodies and succinic acid clearly show a gradual increase along UC severity, except for acetone in UC (Figure 3C for CD and Figure 4B for UC). On the other hand, some amino acids showed a gradually decrease upon increase of disease severity (ie, histidine and lysine). Interestingly, the lower the disease severity is, the higher the concentration of N,N-dimethylglycine is.

The different disease location subgroups included (1) L1 (ileal) + L4 (ileal and upper intestinal), (2) L2 (colonic), and (3) L3 (ileocolonic) for CD; and (1) E1 (proctitis), (2) E2 (left sided), and (3) E3 (extensive) for UC (Figure 3B for CD and Figure 4A for UC). Differential metabolites in each location are shown in Table 2. Among the 3 CD locations, the ileocolonic disease showed the greatest differential metabolite profile in both matrixes. Notably, the 3 ketone bodies, creatine, N,N-dimethylglycine, and succinic acid, showed potential for the discrimination of ileocolonic CD from ileal/upper intestinal

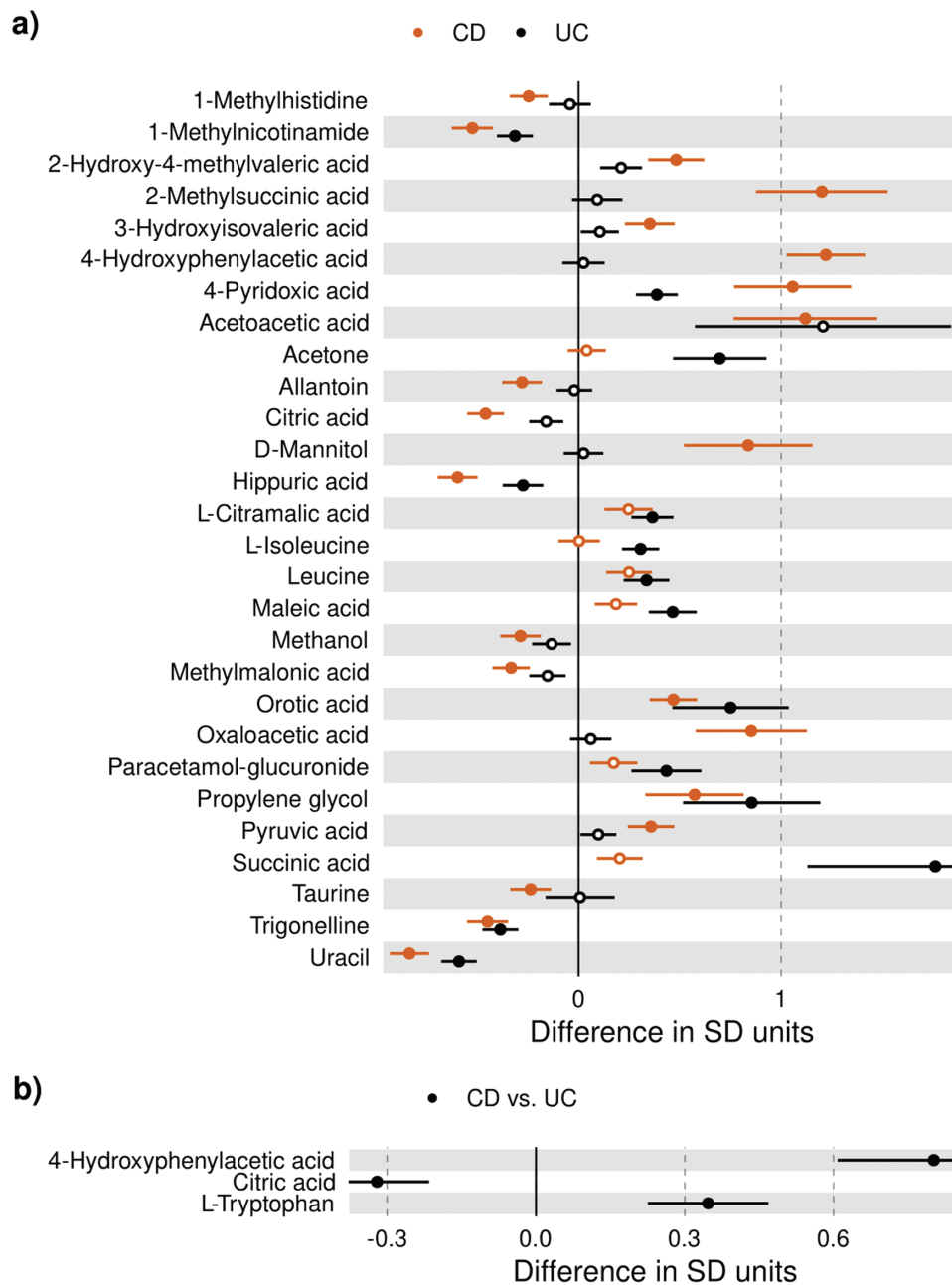


Figure 2. Changes in urinary metabolites (A) in Crohn's disease (CD) and ulcerative colitis (UC) patients compared with healthy control individuals and (B) in CD compared with UC. The horizontal axis is the number of standard deviations (SDs) that a metabolite is on average increased (or decreased) in CD compared with UC. Circles are positioned in the specific mean increase (decrease) value, whereas horizontal black bars are the 95% confidence interval. Statistically significant differences (P value $< .05$) are represented with filled circles.

and colonic CD (standard deviation higher than 2 units). In urine, it is noteworthy that N,N-dimethylglycine was highly significantly increased in ileocolonic CD compared with HC individuals with a difference in standard deviation units >6 , whereas no differences were found in the other 2 CD locations. In colonic CD, only acetic acid in serum and dihydrothymine in urine showed a discriminative potential. For an ileal and/or upper intestinal location, a less discriminative pattern, with small differences in standard deviation compared with HC individuals, was detected (Table 2 and Figures 4B and 5B).

Most of the differential metabolites among UC locations were found in extensive UC (Figure 4A for serum and Figure

6A for urine). Among the 3 UC locations, ketone bodies and succinic acid were highly increased only in extensive UC patients compared with HC individuals and with a wide difference with proctitis and left-sided UC.

As for the CD phenotype, penetrating CD exhibited highly abundant metabolites compared with HC individuals, as well as with inflammatory or stricturing CD, including ketone bodies, amino acids, and succinic acid. On the contrary, new onset inflammatory CD showed none or small difference from HC individuals for almost all the metabolites analyzed (Figures 3A and 5A). In urine, the stricturing CD showed 2 cell membrane components significantly increased namely

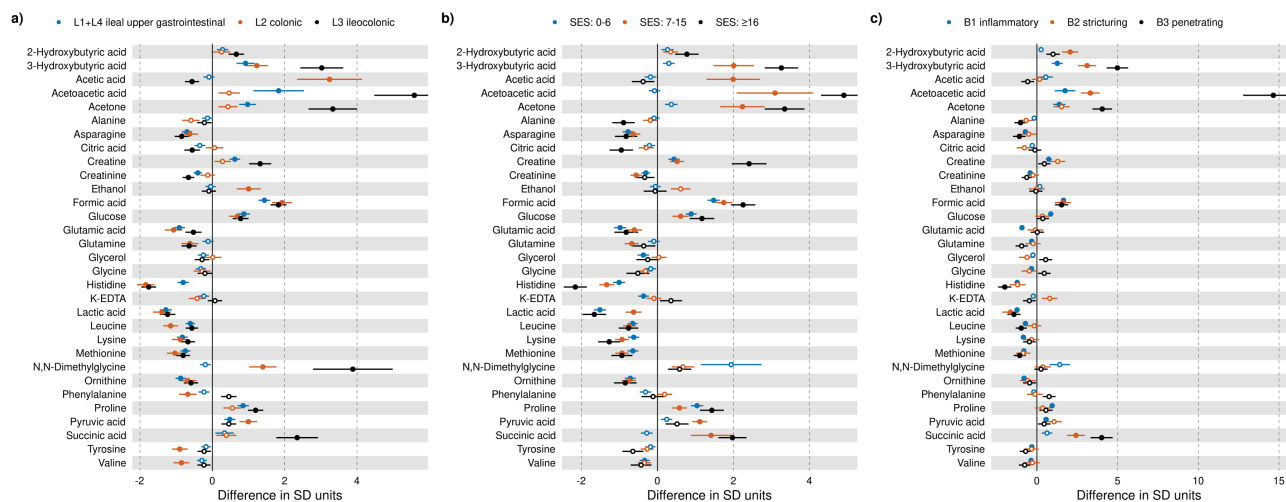


Figure 3. Changes in serum metabolites in Crohn's disease subtypes based on disease (A) severity, (B) location, and (C) phenotype, compared with healthy control individuals. The horizontal axis is the number of standard deviations (SDs) that a metabolite is on average increased (or decreased) in Crohn's disease subtypes compared with healthy control individuals. Circles are positioned in the specific mean increase (decrease) value, whereas horizontal black bars are the 95% confidence interval. Statistically significant differences (P value $<.05$) are represented with filled circles. SES, Simple Endoscopic Score.

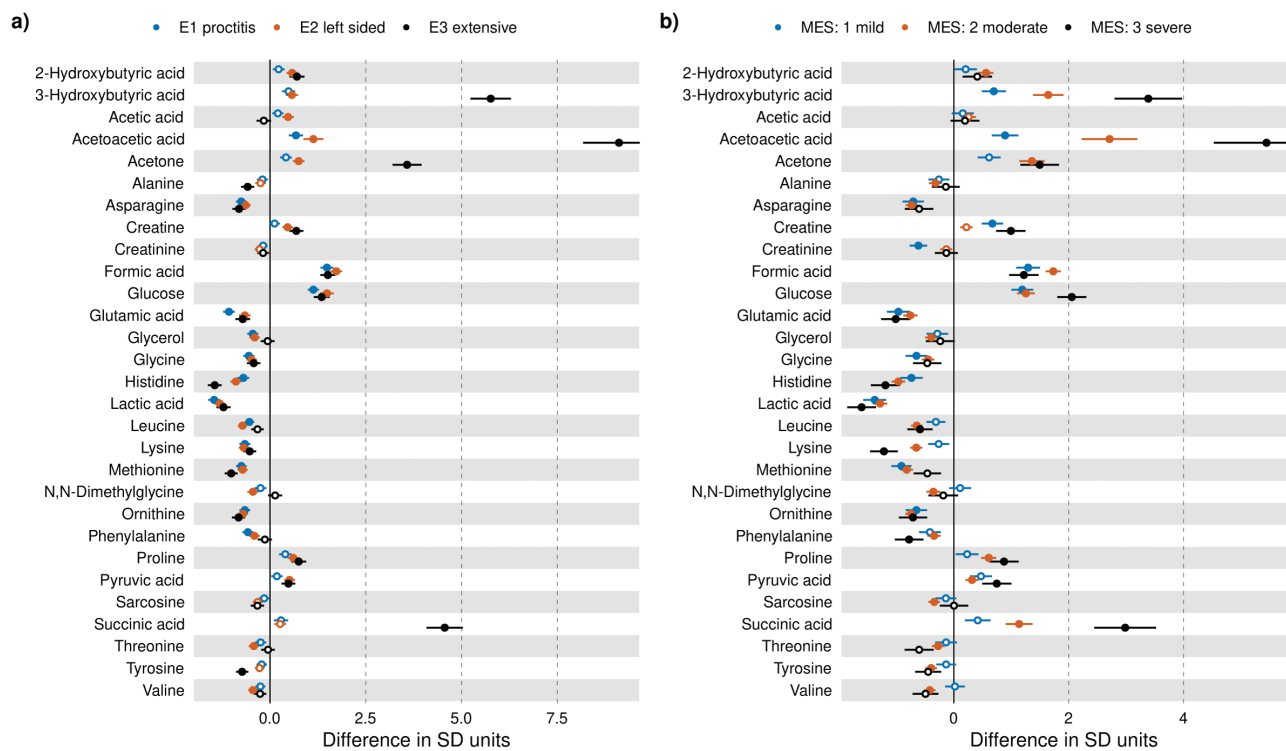


Figure 4. Changes in serum metabolites in ulcerative colitis subtypes based on disease (A) severity and (B) location, compared with healthy control individuals. The horizontal axis is the number of standard deviations (SDs) that a metabolite is on average increased (or decreased) in ulcerative colitis subtypes compared with healthy control individuals. Circles are positioned in the specific mean increase (decrease) value, whereas horizontal black bars are the 95% confidence interval. Statistically significant differences (P value $<.05$) are represented with filled circles. MES, Mayo endoscopic score.

myo-inositol and choline, which could explain the pathological mechanism involved in the disease.

Metabolomic and Clinical Data Integration for Clustering Analysis

We also aimed to establish new IBD subgroups without the previous definition CD or UC. PCA was applied to z -scored clinical and anthropometric data of patients with IBD only to

identify those components that explain the variance observed in the dataset. Then, a simplified PCA derived data matrix of the original clinical and anthropometric data explaining at least 80% of the variance in the original data was constructed for subsequent hierarchical clustering analysis. Clustering at height 9 recovered 3 distinct clusters: cluster 1 ($n = 17$, 53% UC), cluster 2 ($n = 59$, 69% UC), and cluster 3 ($n = 81$, 49% UC) (Figure 7A). Projection of the identified

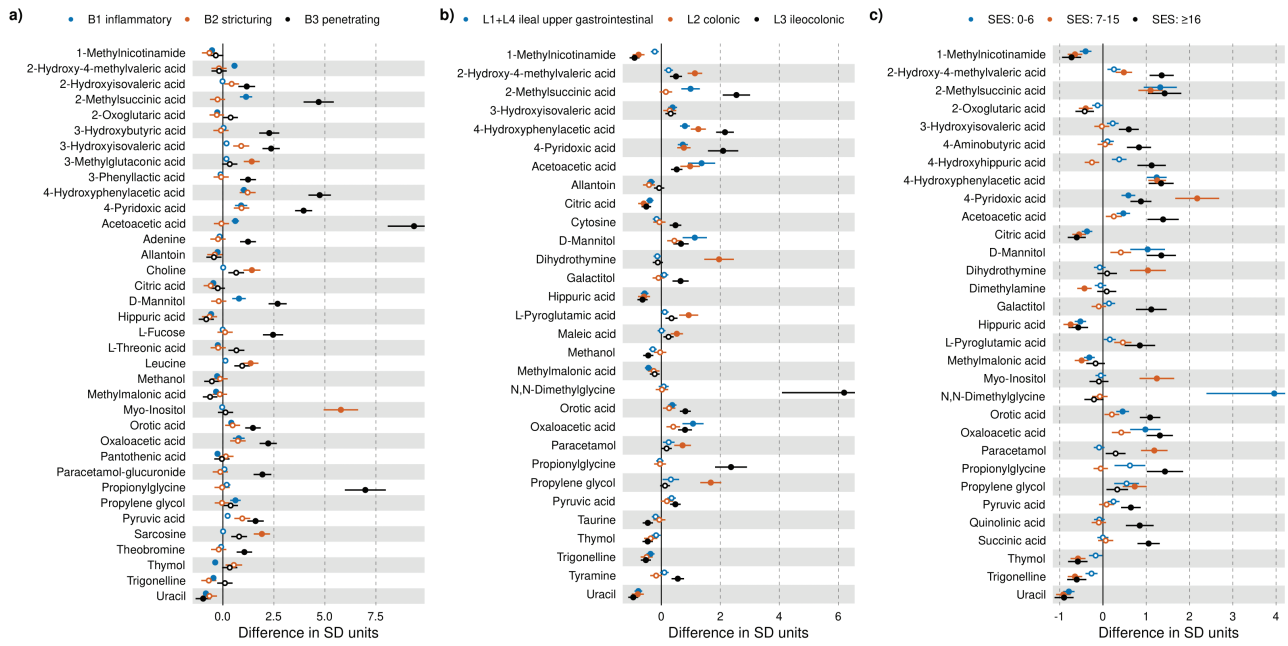


Figure 5. Changes in urinary metabolites in Crohn's disease subtypes based on disease (A) severity, (B) location, and (C) phenotype, compared with healthy control individuals. The horizontal axis is the number of standard deviations (SDs) that a metabolite is on average increased (or decreased) in Crohn's disease subtypes compared with healthy control individuals. Circles are positioned in the specific mean increase (decrease) value, whereas horizontal black bars are the 95% confidence interval. Statistically significant differences (P value $<.05$) are represented with filled circles. SES, Simple Endoscopic Score.

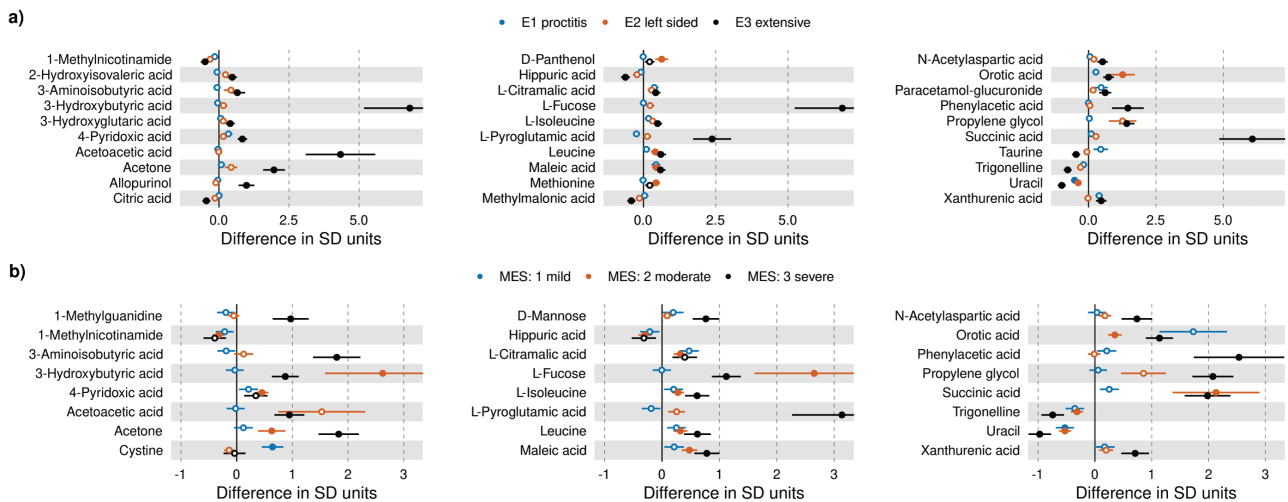


Figure 6. Changes in urinary metabolites in ulcerative colitis subtypes based on disease (A) severity and (B) location, compared with healthy control individuals. The horizontal axis is the number of standard deviations (SDs) that a metabolite is on average increased (or decreased) in ulcerative colitis subtypes compared with healthy control individuals. Circles are positioned in the specific mean increase (decrease) value, whereas horizontal black bars are the 95% confidence interval. Statistically significant differences (p value $<.05$) are represented with filled circles. MES, Mayo endoscopic score.

clusters along the first 2 principal components of the PCA (27.25% and 14.86% for principal components 1 and 2, respectively) allowed for a clearer visualization of the spatial disposition of samples per cluster (Figure 7B). Once clinical subphenotypes had been obtained, mean analyses of the clinical and anthropometric differences among clusters and with respect to HC individuals were conducted and are reported in Table 3.

Orthogonal projections to latent structures discriminant analysis models have been constructed using the identified clusters as class labels. Quality metrics of the obtained models

are reported in Supplementary Table 3. Overall good fit of metabolomic data to the identified clusters was observed in models discriminating cluster 1 from cluster 2 and cluster 2 from cluster 3, specially using both blood and urine data together, with an R^2Y of 0.661 and 0.636, respectively. Of note, cluster 2 mainly consists of UC patients.

Cluster 1 was characterized by older patients, with high levels of glucose, platelets, and leukocytes and low hemoglobin and hematocrit. It was defined by significantly lower levels of many blood lipoproteins, with respect to cluster 2 and cluster 3.

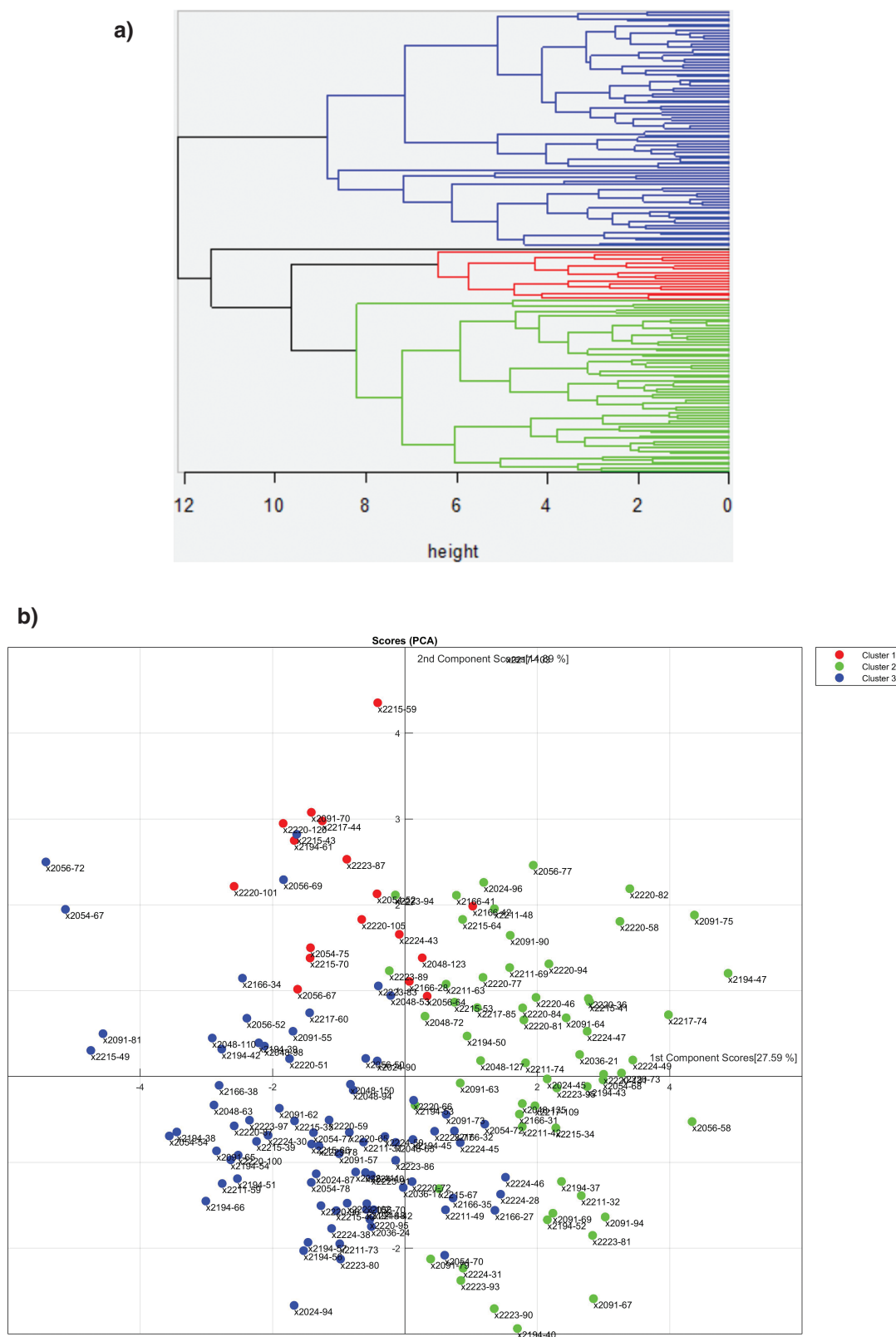


Figure 7. (A) Dendrogram obtained after hierarchical clustering. Cluster 1 is in red, cluster 2 in green, and cluster 3 in blue. (B) Visualization of the obtained clusters after projection onto the first 2 principal components.

Cluster 2 consisted primarily of UC patients, especially extensive UC, with mean values higher than for most metrics, especially weight, hemoglobin, and percentage of hematocrit. It was defined by lower blood levels of high-density

lipoprotein 1 (HDL-1) and HDL-2 TGs and elevated HDL-4 Apo-A2, leucine, methionine, HDL-4 cholesterol, LDL cholesterol/HDL cholesterol, IDL phospholipids, LDL-5 cholesterol, HDL-4 free cholesterol, LDL-5 phospholipids, LDL-5

Table 3. Clinical and anthropometric differences among clusters obtained through clustering.

Variable	Cluster 1 (53% UC)	Cluster 2 (69% UC)	Cluster 3 (49% UC)	Healthy	FDR
Age <i>z</i> score	1.44 ± 0.91	0.40 ± 1.09	-0.51 ± 0.84	-0.02 ± 0.83	<i>a, b, c, x, y, z</i>
Weight <i>z</i> score	0.34 ± 0.64	0.54 ± 0.93	-0.62 ± 0.7	0.07 ± 0.99	<i>b, c, y, z</i>
Height <i>z</i> score	-0.40 ± 0.76	0.37 ± 0.78	-0.36 ± 0.79	0.09 ± 1.04	<i>a, b, c, x, z</i>
BMI <i>z</i> score	0.75 ± 0.94	0.41 ± 0.92	-0.54 ± 0.73	0.03 ± 0.99	<i>a, b, c, y, z</i>
Hemoglobin <i>z</i> score	-1.15 ± 0.77	0.56 ± 0.78	-0.88 ± 0.9	0.32 ± 0.71	<i>a, b, c, x, z</i>
Creatinine <i>z</i> score	-0.40 ± 1.14	0.47 ± 0.94	-0.40 ± 1.13	0.11 ± 0.89	<i>b, c, x, z</i>
Glucose <i>z</i> score	0.82 ± 1	0.30 ± 0.79	-0.30 ± 0.59	-0.20 ± 0.62	<i>a, b, y, z</i>
Cholesterol <i>z</i> score	-0.89 ± 1.03	0.07 ± 1.03	-0.44 ± 0.91	0.28 ± 0.84	<i>a, c, x, z</i>
Triglycerides <i>z</i> score	0.36 ± 0.85	0.22 ± 0.73	-0.22 ± 0.76	-0.04 ± 1	<i>b, z</i>
Hematocrit <i>z</i> score	-1.04 ± 0.62	0.65 ± 0.85	-0.89 ± 0.93	0.28 ± 0.73	<i>a, b, c, x, z</i>
Platelets <i>z</i> score	1.27 ± 1.28	-0.20 ± 0.66	0.71 ± 1.31	-0.31 ± 0.64	<i>a, c, x, z</i>
Leukocytes <i>z</i> score	0.79 ± 1.03	-0.06 ± 0.87	0.20 ± 1.16	-0.17 ± 0.75	<i>a, c, x</i>
ALT <i>z</i> score	-0.22 ± 0.54	0.36 ± 1.06	-0.36 ± 0.6	-0.02 ± 0.84	<i>b, c, x, z</i>
GGT <i>z</i> score	0.17 ± 0.78	0.36 ± 0.77	-0.17 ± 0.55	-0.15 ± 0.48	<i>b, z</i>

Values are mean ± SD. In the table, *a* indicates statistical significance in cluster 1 vs healthy at FDR < 0.05, *b* indicates statistical significance in cluster 2 vs healthy at FDR < 0.05, and *c* indicates statistical significance in cluster 3 vs healthy at FDR < 0.05, *x* indicates statistical significance in cluster 1 vs cluster 2 at FDR < 0.05, *y* indicates statistical significance in cluster 1 vs cluster 3 at FDR < 0.05, and *z* indicates statistical significance in cluster 2 vs cluster 3 at FDR < 0.05.

Abbreviations: ALT, alanine transaminase; BMI, body mass index; CD, Crohn's disease; FDR, false discovery rate; GGT, gamma-glutamyltransferase; UC, ulcerative colitis.

particle number, LDL-5 Apo-B, HDL-4 Apo-A1, LDL-5 free cholesterol, glutamine, and HDL-4 phospholipids with respect to clusters 1 and 3.

Finally, cluster 3 comprised patients with values below the mean across metrics, notably low on hemoglobin and hematocrit percentage but with high levels of platelets and leukocytes. It was characterized by higher levels of blood HDL-1 free cholesterol, HDL-2 cholesterol, and urine oxoglutaric acid, while low levels of blood TGs were also observed.

Discussion

Our results show that at onset, IBD is an inflammatory condition that encompasses profound changes in metabolic homeostasis. Although urine represents an easily accessible biological matrix, our results revealed only marginal differences in a limited number of metabolites. Hence, we focus on serum results in which disturbance in energy and amino acid metabolisms were found in each IBD subgroup, suggesting the increased basal energetic metabolism in IBD patients.

In CD, the metabolomic profile showed altered energy and amino acid metabolic status and a demand of the body for energy, mainly through ketone bodies and the TCA cycle. Ketone bodies together with the observed serum accumulation of TG and LDL-TG are related to fatty acid oxidation-derived acetyl-CoA in the liver, pointing to a reduced hepatic capacity to oxidize acetyl-CoA in the mitochondria, which is then redirected to the synthesis of acetoacetic acid and 2-hydroxybutyric acid.⁹ Consistently with this hypothesis, serum glucose is increased in IBD patients, which could be due to mitochondrial oxaloacetate, which cannot condense with acetyl-CoA to feed the TCA cycle, and is redirected to the cytoplasm into gluconeogenesis, via the synthesis of malic acid. The observed changes in urine of 2-oxo acids (pyruvic acid and oxaloacetic acid), key intermediates in energy

production, reflect the quantities of unused 2-oxo acids in the body that may imply an impairment in energy production. These 2-oxo acids were not altered in UC patients compared with HC individuals.

In UC, the altered metabolite pattern also indicates altered energy and amino acids metabolic status and a demand of the body for energy mainly through the ketone body metabolism. The dramatic increase in succinic acid could indicate defects of the mitochondrial succinate dehydrogenase (SDH) in UC patients. SDH catalyzes the oxidation of succinate to fumarate in the TCA cycle and feeds electrons to the respiratory chain ubiquinone pool.¹⁰ Downregulation of SDH leads to alteration downstream targets for succinate including HIF-1 α and the posttranslational modification of proteins by succinylation.¹¹ In addition, lipopolysaccharide (from Gram-negative bacteria) strongly increases the levels of succinate, which has been demonstrated to promote inflammation by stimulating interleukin (IL)-1 β secretion in murine macrophages through HIF-1 α , thus playing a role in immune responses of these patients.^{12,13} Contrary to our results, succinate has been found significantly decreased in urine in IBD patients.¹⁴⁻¹⁶ Such divergence could be attributed to the onset state and no treatment of our cohort, as most of the studies in the literature analyzed established and treated IBD, besides only UC patients presented higher amount of this TCA acid in urine compared with HC individuals but not with CD patients. In this line, lactic acid has been consistently found increased in established and treated IBD patients,^{15,17,18} but no difference from control individuals was detected in our study. This acid is the end product of glycolysis, and has proinflammatory properties.¹⁹ Moreover, its accumulation in urine may show the lack of lactate-utilizing bacteria that produce mainly butyrate. This difference highlights that even if there is an already existing dysbiosis in onset IBD patients, it is not the same as in established IBD patients, and as expected, the inflammatory status seemed to be less severe in new onset IBD.

Alteration in amino acids in both IBD subgroups has been consistently reported in the literature.^{14,15,20,21} Amino acid alteration has been related to inflammation by inducing oxidative stress and promoting the secretion of proinflammatory cytokines (IL-6, tumor necrosis factor) as well as the migration of peripheral blood mononuclear cells.²² The observed amino acid pattern in both matrices could be reflecting the general metabolic stress and a dysregulated metabolism in the liver. Besides, CD patients showed an alteration in the Trp degradation pathway. Trp is involved in the regulation of immune responses,²³ which may be characteristic of CD etiopathogenesis.

The observed changes indicated that CD has much more marked changes than UC. In this regard, compared with UC, CD presents a more dysbiotic state (higher levels of 4-hydroxyphenylacetic acid and lower hippuric acid and allantoin) and amino acids and energy metabolism highly affected (Trp and citric acid, respectively).

Within CD locations, ileocolonic CD showed an alteration on N,N-dimethylglycine catabolism and an increase in urinary orotic acid and cytosine, which could reveal disruption in nucleotides and amino acid pathways. Overall, gut-derived metabolites exerted a clear significant differential abundance in each CD location.

Extensive UC showed clear changes in cellular energy metabolism and the likely underlying immune response alteration due to the highly increased succinic acid.^{12,13} Gut dysbiosis seemed to be highly present in new onset extensive UC because phenylacetic acid, produced from bacterial degradation of unabsorbed phenylalanine,²⁴ was significantly increased in this phenotype.

Differential metabolites among the 3 severity degrees clearly depicted how differently amino acid metabolism is altered depending on the severity and shows that notwithstanding the CD severity, molecular perturbations are already present. On the contrary, in UC, most of the significant and differential changes occurred in severe UC, and mild or no changes occurred at lower severities. Taken together, our results suggest that metabolomic profile was slightly affected when UC is not severe; however, in CD, even in the mild severities we cannot exclude the possibility of significant metabolic disturbances. In murine models, studies in colitic IL-10^{-/-} mice as well as dextran sulfate sodium colitis-induced mice revealed that differences in metabolite profiles were more profound once as inflammation progresses and colitis is developed.²⁵⁻²⁷

Serum metabolites clearly reflect the highly affected energy and amino acid metabolism in penetrating CD, much more severe than the other 2 phenotypes. Interestingly, the stricturing phenotype showed 2 membrane components significantly increased, namely myo-inositol and choline, which could be involved in the pathological mechanism involved in the disease, as choline is representative of membrane turnover. Moreover, microbiota converts choline to trimethylamine, and its higher excretion suggests a potential gut dysbiosis. Myo-inositol is produced from glucose-6-phosphate and acts as a precursor of inositol phosphates and a cell membrane component.²⁸ Excessive urine myo-inositol could suggest changes in mucosal membrane integrity in these patients as well as renal involvement.

In the clustering analysis, we detected metabolites and lipoproteins that were significantly different among the

defined clusters; however, we did not find relevant phenotypic differences among the clusters.

Although in our cohort study we included a large sample size, which makes the findings valuable, our study has several limitations as well. When subgrouping the different IBD phenotypes, some groups rendered a small sample size, which could affect the statistical power to detect true differences, and thus we note a lack of phenotypic differences among the 3 metabolic clusters. Although several differences were observed among IBD phenotypes, more comprehensive study including other omics (genomics, epigenetics, exposomics, microbial, immunomics, etc.) is needed to obtain a practical clinical application for differential diagnosis or IBD subtype classification. In addition, integrating omics may generate new insight not accessible by any of the individual omics alone, including metabolomics.

Conclusions

The obtained results enlighten the molecular alterations present within the different IBD subgroups at onset. Moreover, the metabolomic profile may provide further understanding of pathogenic mechanisms of IBD subgroups. Alterations in energy and amino acid metabolism, oxidative stress, and inflammatory state occur in newly diagnosed IBD and could further contribute to the development of the different IBD subgroups. Therefore, we speculate that the different metabolomic profiles shed light on putative metabolic changes that occur in new onset IBD as compared with established and treated IBD; thus, the importance of studying these patients without the confounding effect of treatment for understanding the pathological/etiologic mechanism.

The information presented in each IBD subgroup comparison may support diagnosis approaches and provides novel insights into the underlying pathophysiological mechanisms of IBD subgroups, which are far from clear at the present.

Supplementary Data

Supplementary data is available at *Inflammatory Bowel Diseases* online.

Author Contribution

J.P.G., M.C., and L.A.-G. designed the study and wrote the manuscript; S.R., M.R., A.G., I.R.-L., L.F.-S., D.C., J.M.B., M.A., I.B.-R., F.B., M.J.C., R.L., Y.B., D.G., M.E., R.d.F., M.J.G., R.F., A.R.P., B.V., E.G.d.R., S.M.P., A.M.S., M.B.-d.A., A.A., C.V.G., O.R., V.R., M.A., A.G., M.B.-M., C.R., and D.B. participated in patient enrolment and collection of data and approved the final manuscript; R.G.-R., N.E., and O.M. performed the sample analyses and approved the final manuscript; J.J.L., J.S., and A.S.-G. performed bioinformatics, statistical analysis and approved the final manuscript. All authors read and approved the final manuscript. L.A.-G. was the guarantor of the article.

Funding

Financial support obtained through Sara Borrell CD19/00247 and FI17/00143 contracts and PI16/01296 and PI19/01034 projects from the Instituto de Salud Carlos III.

Conflicts of Interest

M.C. has served as a speaker, consultant, or researcher or received education funding from MSD, AbbVie, Hospira, Pfizer, Takeda, Janssen, Ferring, Shire Pharmaceuticals, Dr. Falk Pharma, Tillotts Pharma, Biogen, Gilead, and Lilly. J.P.G. has served as a speaker, consultant, and advisory member for or received research funding from MSD, AbbVie, Pfizer, Kern Pharma, Biogen, Mylan, Takeda, Janssen, Roche, Sandoz, Celgene/Bristol Myers, Gilead/Galapagos, Lilly, Ferring, Faes Farma, Shire Pharmaceuticals, Dr. Falk Pharma, Tillotts Pharma, Chiesi, Casen Fleet, Gebro Pharma, Otsuka Pharmaceutical, Norgine, and Vifor Pharma. M.R. has served as a speaker, consultant, or advisory member for MSD, AbbVie, Pfizer, Takeda, and Janssen. M.-B.-D.A. has served as a speaker, consultant, and advisory member for or received research funding from MSD, AbbVie, Janssen, Kern Pharma, Celltrion, Takeda, Gilead, Celgene, Pfizer, Sandoz, Biogen, Fresenius, Ferring, Faes Farma, Dr. Falk Pharma, Chiesi, Gebro Pharma, Adacyte, and Vifor Pharma. R.L. has served as a speaker or received research or education funding from MSD, AbbVie, Pfizer, Takeda, Janssen, and Dr. Falk. Y.B. has received funding for conference attendance or education from AbbVie, Janssen, and Ferring. M.E. has received support for conference attendance, speaker fees, research support, and consulting fees from AbbVie, Ferring, Janssen, MSD, Otsuka, Pfizer, Takeda, and Tillotts. M.A. has received support for conference attendance from AbbVie, Ferring, Janssen, MSD, Pfizer, Takeda, and Tillotts; and speaker fees from AbbVie and MSD.

Data Availability

The datasets generated during and/or analyzed during the current study are available from the corresponding author on reasonable request.

References

- Kaplan GG. The global burden of IBD: From 2015 to 2025. *Nat Rev Gastroenterol Hepatol*. 2015;12(12):720-727.
- Chaparro M, Zanotti C, Burgueño P, et al. Health care costs of complex perianal fistula in Crohn's disease. *Dig Dis Sci*. 2013;58(12):3400-3406.
- M'Koma AE. Diagnosis of inflammatory bowel disease: Potential role of molecular biometrics. *World J Gastrointest Surg* 2014;6(11):208-219.
- Khan MS, Azmir J. Multi-omics for biomedical applications. *J Appl Bioanal* 2020;6(3):97-106.
- Schoepfer AM, Dehlavi MA, Fournier N, et al.; IBD Cohort Study Group. Diagnostic delay in Crohn's disease is associated with a complicated disease course and increased operation rate. *Am J Gastroenterol*. 2013;108(11):1744-53; quiz 1754.
- Aldars-García L, Gisbert JP, Chaparro M. Metabolomics insights into inflammatory bowel disease: A comprehensive review. *Pharmaceuticals (Basel)* 2021;14(11):1190.
- Bruzzone C, Bizkarguenaga M, Gil-Redondo R, et al. SARS-CoV-2 infection dysregulates the metabolomic and lipidomic profiles of serum. *iScience* 2020;23(10):101645.
- Jiménez B, Holmes E, Heude C, et al. Quantitative lipoprotein subclass and low molecular weight metabolite analysis in human serum and plasma by 1H NMR spectroscopy in a multilaboratory trial. *Anal Chem*. 2018;90(20):11962-11971.
- Newman JC, Verdin E. β -hydroxybutyrate: Much more than a metabolite. *Diabetes Res Clin Pract*. 2014;106(2):173-181.
- Ryan DG, Yang M, Prag HA, et al. Disruption of the TCA cycle reveals an ATF4-dependent integration of redox and amino acid metabolism. *Elife* 2021;10(23):e72593.
- Mills E, O'Neill LAJ. Succinate: A metabolic signal in inflammation. *Trends Cell Biol*. 2014;24(5):313-320.
- Tannahill GM, Curtis AM, Adamik J, et al. Succinate is a danger signal that induces IL-1 β via HIF-1 α . *Nature*. 2013;496(7444):238-242.
- Connors J, Dawe N, Van Limbergen J. The role of succinate in the regulation of intestinal inflammation. *Nutrients* 2019;11(1):25-12.
- Dawiskiba T, Deja S, Mulak A, et al. Serum and urine metabolomic fingerprinting in diagnostics of inflammatory bowel diseases. *World J Gastroenterol*. 2014;20(1):163-174.
- Schicho R, Shaykhtudinov R, Ngo J, et al. Quantitative metabolomic profiling of serum, plasma, and urine by 1H NMR spectroscopy discriminates between patients with inflammatory bowel disease and healthy individuals. *J Proteome Res*. 2012;11(6):3344-3357.
- Stephens NS, Siffledeen J, Su X, Murdoch TB, Fedorak RN, Slupsky CM. Urinary NMR metabolomic profiles discriminate inflammatory bowel disease from healthy. *J Crohns Colitis* 2013;7(2):e42-e48.
- Martin F-P, Su M-M, Xie G-X, et al. Urinary metabolic insights into host-gut microbial interactions in healthy and IBD children. *World J Gastroenterol* 2017;23(20):3643-3760.
- Keshteli AH, Madsen KL, Mandal R, et al. Comparison of the metabolomic profiles of irritable bowel syndrome patients with ulcerative colitis patients and healthy controls: new insights into pathophysiology and potential biomarkers. *Aliment Pharmacol Ther*. 2019;49(6):723-732.
- Haas R, Smith J, Rocher-Ros V, et al. Lactate regulates metabolic and proinflammatory circuits in control of T cell migration and effector functions. *PLoS Biol*. 2015;13(7):e1002202.
- Martin FP, Ezri J, Cominetti O, et al. Urinary metabolic phenotyping reveals differences in the metabolic status of healthy and inflammatory bowel disease (IBD) children in relation to growth and disease activity. *Int J Mol Sci*. 2016;17:1310.
- Alonso A, Julià A, Vinaixa M, et al.; IMID Consortium. Urine metabolome profiling of immune-mediated inflammatory diseases. *BMC Med*. 2016;14(1):133.
- Zhenyukh O, Civantos E, Ruiz-Ortega M, et al. High concentration of branched-chain amino acids promotes oxidative stress, inflammation and migration of human peripheral blood mononuclear cells via mTORC1 activation. *Free Radic Biol Med*. 2017;104:165-177. Epub 13 Jan 2017.
- Opitz CA, Wick W, Steinman L, Platten M. Tryptophan degradation in autoimmune diseases. *Cell Mol Life Sci*. 2007;64(19-20):2542-2563.
- Liu Y, Hou Y, Wang G, Zheng X, Hao H. Gut microbial metabolites of aromatic amino acids as signals in host-microbe interplay. *Trends Endocrinol Metab*. 2020;31(11):818-834.
- Murdoch TB, Fu H, MacFarlane S, Sydora BC, Fedorak RN, Slupsky CM. Urinary metabolic profiles of inflammatory bowel disease in interleukin-10 gene-deficient mice. *Anal Chem*. 2008;80(14):5524-5531.
- Schicho R, Nazzyrova A, Shaykhtudinov R, Duggan G, Vogel HJ, Storr M. Quantitative metabolomic profiling of serum and urine in DSS-induced ulcerative colitis of mice by 1H NMR spectroscopy. *J Proteome Res*. 2010;9(12):6265-6273.
- Lin HM, Barnett MPG, Roy NC, et al. Metabolomic analysis identifies inflammatory and noninflammatory metabolic effects of genetic modification in a mouse model of Crohn's disease. *J Proteome Res*. 2010;9(4):1965-1975.
- Croze ML, Soulage CO. Potential role and therapeutic interests of myo-inositol in metabolic diseases. *Biochimie*. 2013;95(10):1811-1827.